LA-UR-80-2928

CONF-801011--48

TITLE: A COMPARISON OF CALCULATIONAL METHODS FOR EBT REACTOR NUCLEONICS

AUTHOR(S): R. J. Henninger
T. J. Seed
P. D. Soran
D. J. Dudziak

SUBMITTED TO: Fourth Topical Meeting on The Technology of Controlled Nuclear Fusion, October 14-17, 1980, King of Prussia, PA

LOS ALAMOS SCIENTIFIC LABORATORY
Post Office Box 1663 Los Alamos, New Mexico 87545

Form No. 836 R3
St. No. 2629
12/78

UNITED STATES
DEPARTMENT OF ENERGY
CONTRACT W-7405-ENG 36

A COMPARISON OF CALCULATIONAL METHODS FOR EBT REACTOR NUCLEONICS

R. J. Henninger, T. J. Seed, P. D. Soran and D. J. Dudziak
Los Alamos Scientific Laboratory, Los Alamos, New Mexico

Abstract

Nucleonic calculations for a preliminary conceptual design of the first wall/banket/shield/coil assembly for an EBT reactor are described. Two-dimensional Monte Carlo, and one- and two-dimensional discrete-ordinates calculations are compared. Good agreement for the calculated values of tritium breeding and nuclear heating is seen. We find that the three methods are all useful and complementary as a design of this type evolves.

I. Introduction

As the design of a fusion reactor evolves it is important to have confidence in the analysis tools and methods involved in that design process. A part of the design is to provide for the efficient recovery of thermonuclear energy and to shield the superconducting coils. With these goals in mind we have performed various nucleonic analyses of a first wall/blanket/shield/coil configuration as part of a preliminary conceptual design of a reactor based upon the Elmo Bumpy Torus (EBT). The purpose of this paper is to compare and contrast the results obtained by two-dimensional calculations using the continuous-energy Monte Carlo code MCNP[1] and the discrete-ordinates code TRIDENT-CTR[2], and one-dimensional calculations using ONEDANT[3]. The nuclear analysis techniques to be applied to the unique EBT geometry are thus tested for eventual use. The first wall/blanket/shield/coil geometry that will eventually be adopted for further study will differ in composition and dimension from that adopted here. Nevertheless, the methods and procedures described here will be applied in future studies.

In the next section the first wall/blanket/shield/coil design is described. This is followed by sections dealing with Monte Carlo and discrete-ordinates calculations, respectively. In the final sections the results of these calculations are compared and conclusions are drawn about the adequacy of the methods chosen.

II. First Wall/Blanket/Shield/Coil Configuration

A steam/water-cooled Li packed-bed blanket that has been previous analyzed,[4,5] was selected here as a basis for the nucleonic analysis. Figure 1 depicts the geometry used for the nucleonic computations. This configuration has been made cylindrically symmetric to conform with the geometric requirements of the two-dimensional nucleonic model. Table I gives the relevant dimensions, and Tables II and III summarize pertinent dimensions and material compositions of each region. As seen from Fig. 1, the basic calculational unit is one-half of an EBTR sector, of which 42 would exist for the nucleonic/thermohydraulic design selected here. The configuration illustrated in Fig. 1 consists of a conically-shaped plasma chamber surrounded by a 5-mm thick water-cooled stainless-steel first wall and a 0.60-m thick blanket assembly. The blanket has the following functions: a) recover fusion energy in the form of fusion neutrons, secondary gamma rays and first-wall thermal flux, b) breed tritium, and c) act in combination with the shield to reduce to acceptable levels the intensity of the radiation incident on the superconducting magnets. Surrounding the blanket assembly is a 0.68-m thick shield. The shield is separated from the blanket by a 0.29-m thick maintenance void. The shield attenuates the nuclear radiation leaking from the blanket and may serve as a thermal barrier between the blanket and the superconducting magnet coils. The magnet coil assembly is 0.414-m thick and is isolated from the outer edge of the shield by a 0.47-m thick gap at the closest point of contact. The degree to which voids and gaps have been incorporated into this initial estimate of the EBTR blanket/shield/coil configuration has been guided in part by past designs,[6] by the predictions of the magnetics computations[7], and by the desire to maintain an option for additional blanket/shield/structure orientations. The first wall is a "sandwiched" construction of stainless-steel outer regions with a water and stainless-

steel inner region. The blanket assembly is composed of stainless-steel structure, lithium oxide fertile material, water coolant and void. Stainless steel was chosen for the structure because of its availability, ready technology and its compatibility with the lithium oxide over the operating temperature range. Lithium oxide was chosen as the tritium breeding material because of a desire to use existing technologies, such as a direct-cycle steam conversion system[4,5] and a stainless-steel blanket structure. The Li_2O packed bed would be cooled by radial water/steam tubes.

The dimensions and composition of the shield and magnet assemblies are given in Table III. The shield is modelled by 65 v/o steel and 35 v/o borated water, whereas the magnet assemblies consist of a copper matrix surrounded by a stainless-steel jacket (bobbin). On the outside of the magnet assemblies is located a layer of concrete. The torus would be located in this concrete tunnel. The concrete was included in the calculations to model its effect on the heating in the magnet coil assemblies.

Two-dimensional calculations of important thermal and nucleonic responses were made by both Monte Carlo and discrete-ordinates methods. The spatial and angular variation of the 2-D neutron source was determined by an auxiliary Monte Carlo calculation. The results of the Monte Carlo calculation were compared to the predictions of one-dimensional and two-dimensional deterministic calculations. These calculations and the comparisons are described in the following sections.

III. Monte Carlo Model and Calculations

The Monte Carlo nucleonic calculations were performed using the continuous-energy Monte Carlo code MCNP. The nuclear cross-section data were obtained form the RMCCS and MCPL libraries, as described in Ref. 1, and for the most part consist of ENDF/B-IV. Use of continuous-energy cross sections eliminates the approximations associated with a multigroup approach, (e.g., self-shielding effects and weighting functions). All calculations are based on a coupled neutron and photon transport formulation and used the kerma factors from the RMCCS library.

On the basis of the magnetics studies reported in Ref. 7, it was determined that a conical first wall would be superior to a purely cylindrical geometry. Furthermore, since the plasma density varied both in the axial and the radial directions, it was necessary to develop an appropriate description for the spatially-dependent neutron source. Since the model adopted for this nucleonic study consists of 42 sectors arrayed in a toroidal geometry, the number of sectors needed for a representative nucleonic model became a question; differences between the neutron current at the inboard versus the outboard locations of the first wall may also be important. A study was performed to examine the effects of spatial variation of the neutron source, the number of sectors required by the calculation, the differences on the upper and lower first wall and the angular distribution of the outward-bound neutrons on the first wall.

Figure 2 illustrates the results of a Monte Carlo sampling based on an n^2 source distribution and a parabolic density profile. The variation of the neutron wall loading along the toroial axis as a function of the number of sectors included in the calculation is shown, as is the neutron wall loading variations at the inboard versus outboard first-wall locations. In all cases an n^2 source distribution was sampled, the neutrons were transported to the first wall and the total outward-directed uncollided neutron flux was determined on nine conical bands along the toroidal axis for both the inboard and outboard first-wall sections. In studying the required number of sectors, reflecting boundary conditions were established on each end of the sector array. For each case approximately 500 000 points were sampled, and the relative standard deviations were computed to within 1%. Figure 2 shows a $\sim$ 30% variation of neutron flux in the axial direction with virtually no variation in the radial direction because of the cylindrical approximation adopted for the nucleonic model. Futhermore, the results using three and two half sectors are almost identical to those for one half sector, demonstrating that the use of a single half sector for the nucleonic calculation would be sufficient. This conclusion is applied for all subsequent nucleonic calculations.

The angular variation of the neutron flux on the first wall closely follows a $\cos^2\theta$ distribution for the outward-directed neutrons; the angle θ is measured between the normal to the first wall and the neutron direction. This conclusion was also incorporated in the source description for the remainder of this study. All results are normalized to an average neutron wall loading of 1.0 MW/m^2.

The spatial distribution of the tritium breeding is shown in Fig. 3. The radial distance is measured relative to the coil-plane location. Tritium production from ^7Li reactions results from neutrons with energy

greater than ~ 2.5 MeV, which in this case contributes ~ 23% to the total tritium production.

The spatial distribution of the nuclear heating rate in the first wall and blanket assembly is shown in Fig. 4 for a neutron wall loading of 1.0 MW/m^2. The heating rate in each of four axial segments (Fig. 1) is shown. Segment 1 extends from the coil plane to an axial position of 1.2 m segment 2 extends from 1.2 m to 2.23 m, segment 3 extends from 2.23 m to 3.35 m, and segment 4 extends from 3.35 m to the midplane. The radial distance depicted on Fig. 4 is measured relative to the coil plane. Peak heating in the first-wall assembly occurs in segment 4 (9.3 MW/m^3). Peak heating in the blanket assembly also occurs in segment 4 of the first radial cell (5.9 MW/m^3). For the assumed source distribution used in these calculations the axial variation of neutron/gamma-ray heating is acceptable from the viewpoint of thermohydraulics.

Peak heating in the shield assembly occurs in the first shield cell of axial segment 2 (0.16 MW/m^3). The energy deposition rate decreases by over three orders of magnitude through the shield. In the first cell of the magnet assembly the peak heating rate is reduced to 9.2 W/m^3. Figure 5 illustrates the radial distribution of the heating rate in the magnet assembly. Over 90% of the heating in the magnet is generated by the secondary gamma rays produced by thermal neutron captures in the stainless-steel bobbins and the copper stabilizers.

IV. Discrete-Ordinates Models and Calculations

A one-dimensional discrete-ordinate calculation was conducted in parallel to the Monte-Carlo analysis for several purposes. First, consistency checks were performed in the comparative analysis with the Monte Carlo results, providing a confirmation of both the modeling and the results. These comparative calculations proved useful during the debugging of the Monte Carlo calculations. Secondly, the one-dimensional representation of the EBTR blanket/shield/coils configuration provided an opportunity to develop a basis for accuracy estimates in subsequent one-dimensional scoping calculations as the design evolves, including geometric modeling and multigroup effects. It is shown below that for certain nucleonic parameters, such as nuclear heating and tritium breeding, the one-dimensional results are remarkably close to the two-dimensional Monte Carlo and discrete-ordinates results. Lastly, the one-dimensional results provide detailed radial distributions of response rates; these data are not inherently available from a Monte Carlo analysis. All one-dimensional analyses were performed with the discrete-ordinates code ONEDANT,[3] using an S_8 angular quadrature and P_3 scattering matrices. The standard LASL 30 neutron and 12 gamma-ray energy-group structure was employed; cross-section data are derived from ENDF/B-IV via the MATXS library at the NMFECC.

A one-dimensional traverse through the conical blanket/shield (Fig. 1) was selected at average plasma and first-wall radii of 1.09 and 1.14 m, respectively. Continuing radially through the outer steel shield structural support to a radius of 2.69 m, the traverse shifted axially and then was taken radially through the TF coil and its associated steel supports (bobbins) and concrete backing. Because the design shown in Fig. 1 is effectively two-dimensional, the neutron source was averaged over the 4.47-m half-sector length to give exactly the same number of 14.1-MeV neutrons emitted over the half-sector length. Because the first-wall areas differ between the conical walls of the Monte Carlo model and the cylindrical walls used in the one-dimensional discrete-ordinates model, the neutron wall loadings, I_w, were 1.0 and 1.06 MW/m^2, respectively.

Figure 6 shows the spatial distributions of neutron and gamma-ray heating computed by ONEDANT for all regions. Similarly, Fig. 7 shows the spatial distribution of tritium breeding.

For the geometry depicted in Fig. 1, two-dimensional discrete-ordinates calculations were made by means of the TRIDENT-CTR code. The TRIDENT-CTR calculations were performed in S_4-P_3 and S_4-P_1 modes, using the same 42-group cross-section set as in ONEDANT. The spatial and angular distributions of plasma neutrons at the first wall were used as a surface source for the TRIDENT-CTR calculations. This first-wall distribution was the same as that used in the Monte Carlo calculations.

V. Comparison of Nucleonic Responses

A major response of interest in any fusion power reactor concept is tritium breeding. At this stage of the design effort neither the Monte Carlo (MCNP) nor discrete-ordinates (ONEDANT and TRIDENT-CTR) calculations include any streaming paths in ducts for plasma heating or vacuum pumping systems, so some margin is required above a tritium breeding ratio of unity. Also, considering that ~ 23% of the tritium breeding ratio is due to ^7Li (n,n't) ^4He reactions, the evidence[8] that this reaction cross-section is at least 15% over-estimated in the ENDF/B data files requires a further breeding margin

above unity. Final results for ONEDANT, TRIDENT-CTR (P_3), TRIDENT-CTR (P_1), and MCNP are, respectively, breeding ratios of 1.174, 1.168, 1.168 and 1.169. Similarly, DT-neutron energy multiplications of 1.19, 1.18, 1.18 and 1.15, respectively, were found. Table IV presents selected values of nuclear heating from the four calculations. It can be seen that all four calculations agree as to the breeding ratio and the energy recovery in the shield and blanket regions. Differences in the first-wall heating rate can be explained by differences between the 1-D and 2-D source distributions. The 2-D source neutrons were more peaked in the outward direction. This led to the determination of fewer first-wall interactions by the TRIDENT-CTR and MCNP calculations. With the exception of the TRIDENT-CTR (P_1) calculation, the agreement between nuclear heating values in the coils is remarkably good, considering the large attenuation of neutron and gamma-ray flux through the blanket/shield (of order 10^6). The close agreement in integral quantities such as total tritium breeding and total energy deposition is due in part to the fact that cross sections and kerma factors were in all cases derived mostly from ENDF/B-IV data processed by the NJOY code[9]. The ONEDANT and Monte Carlo calculations indicate that the shield is adequate to meet a criterion of $< 10^{-5}$ MW/m^3 in the inner coil supports. The detailed spatial distributions of nuclear heating and tritium breeding, as computed by TRIDENT-CTR with a P_3 approximation, are shown in Figs. 8-10, where the contours represent isoresponse levels. Figure 9 shows the total (neutron plus gamma-ray) heating in the TF coil, coil supports and concrete backing The contours shown are given in equal logorithmic decrements, with the maximum value of $\sim 10^{-5}$ MW/m^3 occurring at the surface facing the blanket radially, and at the axial end of the coil. The latter location of relatively high heating rates indicates the importance of radiation from the shield and concrete, which enters the coil at its axial surface. Based upon this result, further refinements of this preliminary conceptual design, such as local shielding around the coil, should be considered.

VI. Conclusions

From the foregoing analysis we can draw several conclusions. First, the 1-D modeling appears to provide a very acceptable level of accuracy in predicting tritium breeding and nuclear heating (with the possible exception of the first wall), despite the conical wall geometry and non-uniform D-T neutron source distribution. The close agreement between the Monte Carlo and the three discrete-ordinates calculations of tritium breeding and heating also implies that resonance self shielding is not an important effect in this design. Also, the comparison with continuous-energy Monte Carlo calculations again confirms the adequacy of the 42-group energy structure used in the discrete-ordinates analysis. Likewise, confidence was gained in the adequacy of a P_3 angular scattering approximation and an S_4 angular quadrature. Finally, we have seen that detailed 2-D contour plots from TRIDENT-CTR, not inherently available in Monte Carlo calculations, are useful as the design evolves.

References

1. LASL Group X-6, "MCNP-A General Monte Carlo Code for Neutron and Photon Transport," Los Alamos Scientific Laboratory report LA-7396-M (Revised) (1979).

2. T. J. Seed, "TRIDENT-CTR User's Manual," Los Alamos Scientific Laboratory report LA-7835-MS (1979).

3. R. D. O'Dell, F. W. Brinkley, Jr. and D. R. Marr, "User's Manual for ONEDANT: A Code Package for One-Dimensional, Diffusion-Accelerated, Neutral-Particle Transport," Los Alamos Scientific Laboratory report in preparation.

4. R. L. Hagenson and R. A. Krakowski, "The Reversed-Field Pinch Reactor (RFPR) Concept," Los Alamos Scientific Laboratory report LA-7973-MS (1979).

5. G. E. Cort, R. L. Hagenson and R. A. Krakowski, "A Direct-Cycle Steam Generating Blanket Design," Trans. Amer. Nucl. Soc, 33, 76 (1979).

6. D. G. McAlees, N. A. Uckan, E. S. Bettis, C. L. Hedrick, E. F. Jaeger and D. B. Nelson, "The Elmo Bumpy Torus Reactor (EBTR) Reference Design," Oak Ridge National Laboratory report ORNL/TM-5669 (November 1976).

7. R. A. Krakowski, C. G. Bathke et al., "The Reassessment of the Elmo Bumpy Torus Reactor Concept: Phase I, Physics Design," Los Alamos Scientific Laboratory report (to be published).

8. D. J. Dudziak and G. L. Woodruff, "Nucleonic Aspects of Synfuel Blankets," Los Alamos Scientific Laboratory report LA-7485-MS (1978).

9. R. E. MacFarlane, R. J. Barrett, D. W. Muir, and R. M. Boicourt, "The NJOY Nuclear Data Processing System: User's Manual," Los Alamos Scientific Laboratory report LA-7584-MS (1978).

TABLE I

EBTR DESIGN PARAMETERS USED FOR PRELIMINARY BLANKET/SHIELD NUCLEONIC CALCULATIONS

PARAMETER	VALUE
Major radius, R_T(m)	60.0
First-wall radius, r_w(m)	0.91[a]
First-wall thickness, (mm)	5.0
Blanket thickness, (m)	0.6
Maintenance void, (m)	0.29
Shield thickness, (m)	0.68
TF-coil inner radius, r_c(m)	3.20
TF-coil thickness, (m)	0.41
TF-coil length, (m)	2.40
Concrete biological shield thickness, (m)	0.40
Half-sector length, (m)	4.47
Plasma volume, (m^3/half sector)	20.78
First-wall area, (m^2/half sector)	34.10
Number of sectors, N	42
Average neutron wall loading, I_w(MW/m^2)	1.0

(a) radius at coil plane, which increases to 1.5 m at the midplane for the conical first wall.

TABLE II

BLANKET ASSEMBLY MATERIALS AND DIMENSIONS

ITEM	OUTER RADIUS (m)[a]
First wall[b]	0.9120
Water coolant[c]	0.9140
First wall	0.9150
Blanket structure[b]	0.9483
Blanket[d]	0.9830-1.4569[e]
Blanket structure[b]	1.5100

(a) measured at coil plane, first wall radius is 0.91 m

(b) SS-2.5 w/o Cr; 1.3 w/o Mo; 96 w/o Fe

(c) 34 v/o SS and 66 v/o H_2O

(d) 15 v/o SS; 40 w/o Li_2O; 10 v/o H_2O and 35 v/o void

(e) blanket divided into 12 radial units.

TABLE III

DIMENSIONS AND COMPOSITIONS OF THE SHIELD AND MAGNET COILS

ITEM	MATERIAL	LENGTH (m)	THICKNESS (m)
Shield Assembly			
· Structure	SS[a]	Full[b]	0.038
· Shielding material	SS + H_2O + H_3BO_3[c]	Full	0.517
· Structure	SS[a]	Full	0.116
Shield-magnet Separation (at the closest contact point)	void		0.47
Magnet coil assembly			
· Bobbin	SS[a]	1.202	0.05
· Coil	Cu	1.202	0.26
· Bobbin	SS[a]	1.202	0.10
Biological shield	Concrete[d]	Full	0.40

(a) 2.5 w/o Cr; 1.5 w/o Mo; 96.0 w/o Fe

(b) Full length of the one-half sector is 4.47 m

(c) 65 v/o SS[a] and 35 v/o borated water, borated water: 12 w/o H_3BO_3, 19.78 a/o ^{10}B.

(d) Concrete composition (all weight percents): ^1H (0.477); O(60.408) Na (0.947); Mg (0.3); Al (2.482); Si (24.187); K (0.685); Ca (2.048); Fe (0.465). Density: $2.25(10)^3$ kg/m^3.

TABLE IV

COMPARSION OF SELECTED NUCLEAR HEATING RATES[a]

		TOTAL NUCLEAR HEAT (MW/m) and [% OF TOTAL]			
REGION	THICKNESS(m)	ONEDANT	MCNP	TRIDENT-CTR (P_3)	TRIDENT-CTR (P_1)
FIRST WALL	0.005	0.38[4.2]	0.32[3.6]	0.32[3.7]	0.33[3.7]
BLANKET	0.59	8.40[93.4]	8.22[93.7]	8.42[94.2]	8.43[94.1]
SHIELD	0.671	0.21[2.4]	0.23[2.6]	0.19[2.17]	0.20[2.2]
INNER COIL SUPPORT	0.051	$9.78(10)^{-6}$[$3.0(10)^{-5}$]	$8.63(10)^{-6}$[$2.6(10)^{-5}$]	$11.8(10)^{-6}$[$3.5(10)^{-5}$]	$13.3(10)^{-6}$[$4.0(10)^{-5}$]
TF COIL	0.264	$2.27(10)^{-5}$[$6.8(10)^{-5}$]	$2.22(10)^{-5}$[$6.7(10)^{-5}$]	$2.34(10)^{-5}$[$7.0(10)^{-5}$]	$2.62(10)^{-5}$[$7.9(10)^{-5}$]
ALL REGIONS	1.876	8.99	8.77	8.94	8.96

(a) Based upon neutron wall loading 1 MW/m^2 on conical wall in MCNP and TRIDENT-CTR calculations. ONEDANT equivalent wall loading is 1.06 MW/m^2.

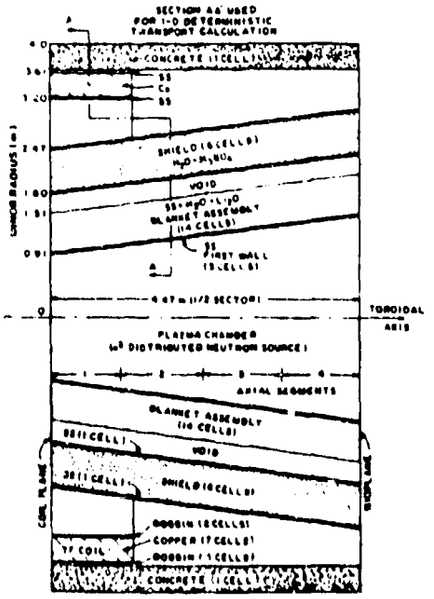

Fig. 1. Nucleonic model used for two-dimensional representation of First-wall/Blanket/Shield/Coil Geometry.

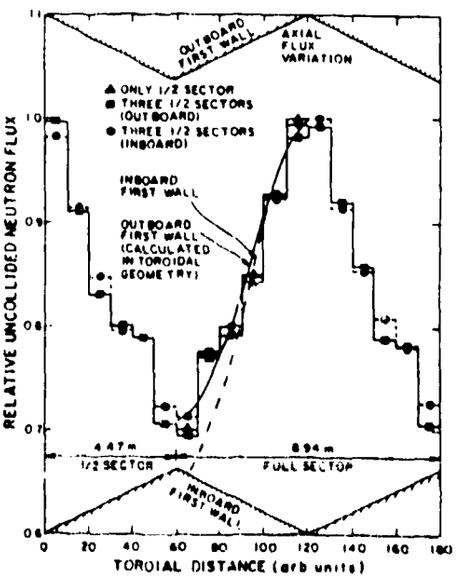

Fig. 2. Toroidal dependent of neutron wall loading at inboard and outboard regions as a function of number of halfsectors included. Shown also is the prediction of an analytic (toroidal) model (Ref. 7) with both inboard and outboard results being normalized separately.

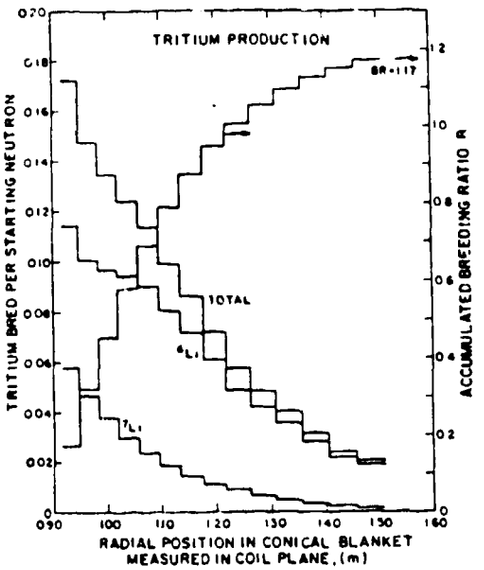

Fig. 3. Radial dependence of axially-integrated tritium breeding measured relative to coil-plane location for blanket sub-regions of varying width.

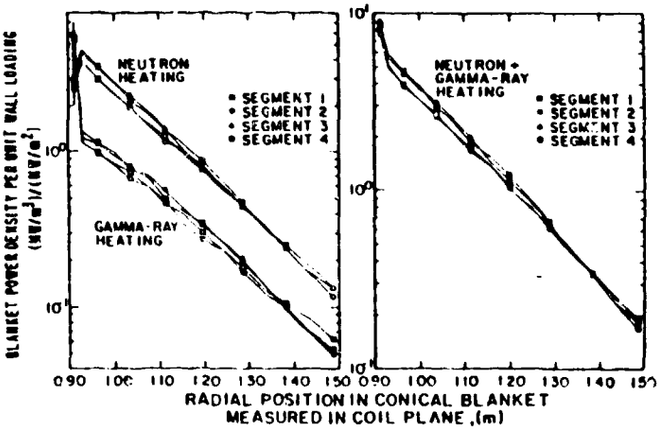

Fig. 4. Radial variation of axially-integrated neutron and gamma-ray heating measure relative to coil-plane location.

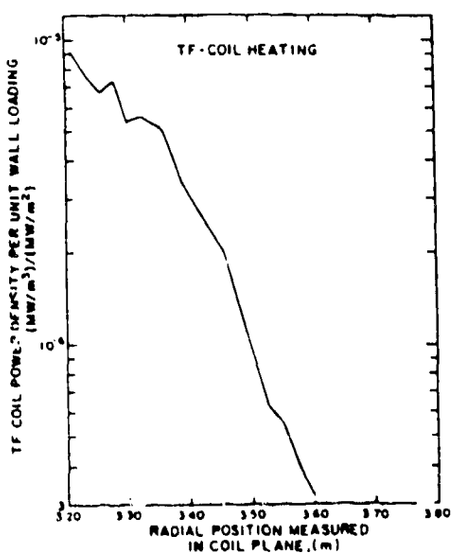

Fig. 5. Radial dependence of nuclear heating in superconducting TF coil.

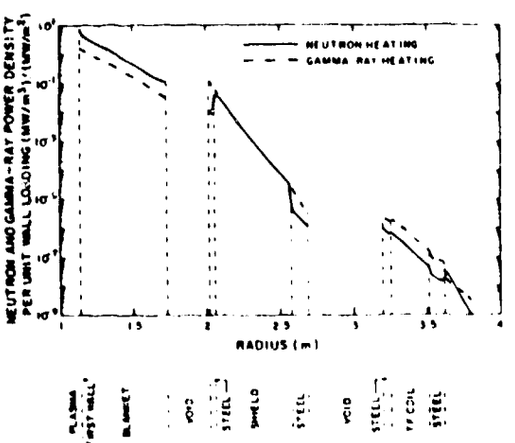

Fig. 6. Spatial distribution of neutron and gamma-ray heating determined by a one-dimensional (radial) transport model, ONEDANT.

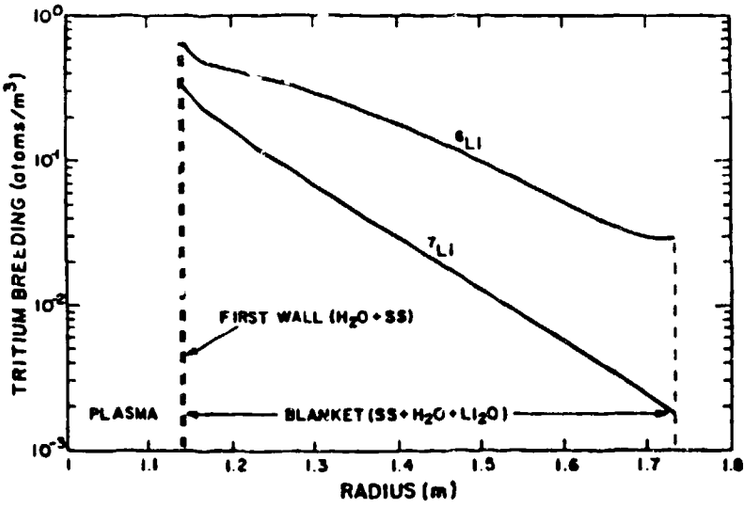

Fig. 7. Spatial distribution of tritium breeding determined by a one-dimensional (radial) transport model, ONEDANT, based upon a unit neutron source per meter of plasma length.

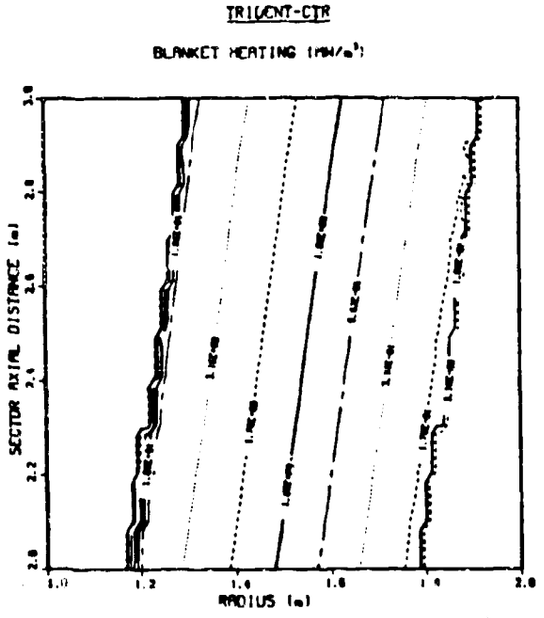

Fig. 8. Nuclear heating profiles in blanket as determined by TRIDENT-CTR.

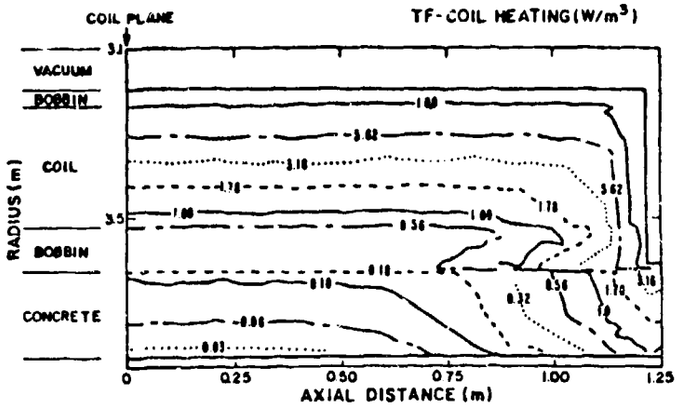

Fig. 9. Nuclear heating profile in TF coil as determined by TRIDENT-CTR.

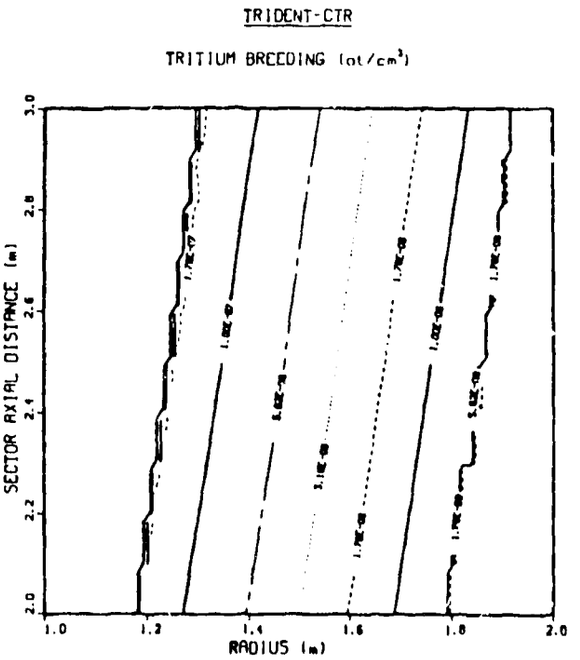

Fig. 10. Tritium breeding profiles in blanket as determined by TRIDENT-CTR.